Fabry-Perot interference and spin filtering in carbon nanotubes

Claudia S. Peça and Leon Balents

Physics Department, University of California, Santa Barbara, CA 93106

Kay Jörg Wiese

Kavli Institute for Theoretical Physics, University of California, Santa Barbara, CA 93106

(Dated: April 22, 2003)

We study the two-terminal transport properties of a metallic single-walled carbon nanotube with good contacts to electrodes, which have recently been shown [W. Liang et al, Nature 441, 665-669 (2001)] to conduct ballistically with weak backscattering occurring mainly at the two contacts. The measured conductance, as a function of bias and gate voltages, shows an oscillating pattern of quantum interference. We show how such patterns can be understood and calculated, taking into account Luttinger liquid effects resulting from strong Coulomb interactions in the nanotube. We treat back-scattering in the contacts perturbatively and use the Keldysh formalism to treat non-equilibrium effects due to the non-zero bias voltage. Going beyond current experiments, we include the effects of possible ferromagnetic polarization of the leads to describe spin transport in carbon nanotubes. We thereby describe both incoherent spin injection and coherent resonant spin transport between the two leads. Spin currents can be produced in both ways, but only the latter allow this spin current to be controlled using an external gate. In all cases, the spin currents, charge currents, and magnetization of the nanotube exhibit components varying quasiperiodically with bias voltage, approximately as a superposition of periodic interference oscillations of spin- and charge-carrying "quasiparticles" in the nanotube, each with its own period. The amplitude of the higher-period signal is largest in single-mode quantum wires, and is somewhat suppressed in metallic nanotubes due to their sub-band degeneracy.

PACS numbers: 73.63.-b,71.10.Pm,72.25.-b

I.   INTRODUCTION

Spin transport represents a new branch in mesoscopic physics with several technological applications[1,2,3,4,5,6], e.g. information storage, magnetic sensors and potentially quantum computation[7]. While most theoretical models are based on Fermi liquid theory, some work has been done on strongly correlated 1D systems using Luttinger liquid theory[8,9,10,11,12]. This work has focused in the weak tunneling regime between the ferromagnet and the 1D system and found that spin transport may provide experimental evidence of spin charge separation, one of the main predictions of Luttinger liquid theory that remains to be observed experimentally in an unambiguously accepted way. Despite the possible technological applications and contributions to the study of spin charge separation in strongly correlated systems, very little experimental work has been carried out on spin transport in 1D systems.[13] This work is complicated by the use of multi-walled carbon nanotubes, and explored only situations with ferromagnetic contacts with parallel or antiparallel magnetizations.

Early experimental work with nanotube devices was limited by poor contacts between the electrodes and the nanotube, and accordingly theoretical models focused in the weak tunneling regime. Recently, Liang *et al.*[14] have succeeded in fabricating single-walled carbon nanotube devices with near-perfect ohmic contacts to the electrodes. A schematic representation of their experiment is presented in Fig. 1. These devices are characterized by values of the conductance as high as $G = 3.7e^2/h$, close

to the theoretically predicted higher limit[15] of $4e^2/h$. At temperatures below 10K, the measured conductance exhibits approximately periodic oscillations as a function of the gate voltage. These oscillations are due to Fabry-Perot interference – i.e. quantum interference between propagating electron waves inside the resonant cavity defined by the two nanotube-electrode interfaces. In order to explain their result, Ref. 14 considered a model of non-interacting electrons and used the multi-channel Landauer-Büttiker formalism to calculate the differential conductance as a function of the bias and gate voltages. They have found qualitative agreement between the calculated conductance and their experimental data, especially with regard to the variation of the low-bias conductance with gate voltage.

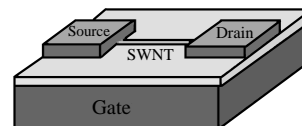On the other hand, transport experiments on carbon

FIG. 1: Experimental geometry (from Ref. 14). A single-walled carbon nanotube is located on a silicon gate and oxide layer. The electrodes, which may be ferromagnetic, are grown on top of the nanotube. The doped silicon is used as a gate electrode to modulate the charge density. The electronic transport properties of the nanotube devices were characterized as a function of bias (V) and gate (V_g) voltages.

nanotubes[16,17,18,19] have shown that electrons in nanotubes are strongly correlated and are better described by a Luttinger liquid model[20,21,22,23,24,25]. This implies the electrons in these systems do not exhibit Fermi liquid properties but instead form collective excitations better described by charge and spin like density waves that propagate with different velocities. This Luttinger liquid behavior drastically changes the charge conductance for these systems and it is interesting to know how this affects the results obtained for the particular setup used in Ref. 14. Furthermore, this setup can be generalized to the use of ferromagnetic electrodes, in order to study both charge and spin transport in 1D electron systems.

In this paper we investigate the spin and charge transport properties in 1D electron systems with near-perfect contacts to ferromagnetic electrodes (the normal metal electrodes correspond to the particular case of zero magnetization). We consider both the case of quantum wires, i.e. single-channel electron systems, and single-walled carbon nanotubes, but mainly focus on the latter one. We use a non-interacting Stoner model to treat the ferromagnetic leads and a Luttinger liquid model for the nanotube and consider the case of near-perfect contacts to the leads, therefore treating backscattering at the contacts perturbatively. In order to introduce the effect of a finite bias voltage, we use the non-equilibrium Keldysh formalism. Following this procedure, we obtain the conductance, spin and spin current as functions of the gate and bias voltages, the external magnetic field and the orientation of the magnetization in each lead. We study how the strong Coulomb interactions affect these transport properties and find some features in the Fabry-Perot interference patterns that are related to spin charge separation.

II. THE MODEL

A single-walled carbon nanotube with long-range Coulomb interactions is well described by a forward-scattering model[24,25]. In this model the Hamiltonian density is given by

$$
\begin{aligned}
\mathcal{H}_{\mathrm{LL}} &= -iv_{\mathrm{F}} \sum_{a=1}^{2} \sum_{\alpha=\uparrow,\downarrow} \left(\psi_{Ra\alpha}^{\dagger} \, \partial_x \psi_{Ra\alpha} - \psi_{La\alpha}^{\dagger} \, \partial_x \psi_{La\alpha} \right) \\
&+ \lambda \left[\sum_{a=1}^{2} \sum_{\alpha=\uparrow,\downarrow} \left(\psi_{Ra\alpha}^{\dagger} \, \psi_{Ra\alpha} + \psi_{La\alpha}^{\dagger} \, \psi_{La\alpha} \right) \right]^2 , \quad (1)
\end{aligned}
$$

where the right/left moving electron operators $\psi_{R/L\,a\alpha}$ have the labels $a = 1, 2$ for the band and $\alpha = \uparrow, \downarrow$ for the spin projection of the electrons in the nanotube and λ is the interaction strength. The term in the square brackets corresponds to the electron density. We also consider the same problem for a single-channel quantum wire, for which there is no sub-band degeneracy and the band index can be dropped. Due to the similarities between the
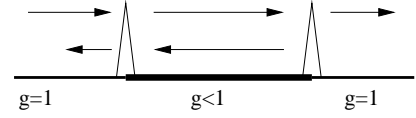

FIG. 2: Schematic representation of the model. The leads are modeled as 1D non-interacting electron systems, the Luttinger liquid parameter is therefore $g = 1$. The nanotube (bold line), on the other hand, is described by a 1D interacting system, in this case $g < 1$, which corresponds to repulsive interactions. The contacts to the leads are modeled as two weak backscattering barriers. The two backscatterers generate Fabry-Perot interference.

two cases, we give explicit analytical formulas throughout the paper only for the nanotube, but will present results for the quantum wire where appropriate.

The metallic leads are modeled as two semi-infinite 1d-non-interacting systems[26,27,28], which is obtained with a position dependent λ, constant in the wire and zero in the leads.

We allow for ferromagnetism in the leads using a non-interacting Stoner model[8,9] (mean-field treatment of the magnetization). The Hamiltonian density is $\mathcal{H}_{\mathrm{FM}} = \mathcal{H}_0 + \mathcal{H}_M$ with $\mathcal{H}_0 = \mathcal{H}_{LL}(\lambda = 0)$ and

$$
\mathcal{H}_M = -\vec{M} \cdot \sum_{a\alpha\beta} \left(\psi_{Ra\alpha}^{\dagger} \, \vec{\sigma}_{\alpha\beta} \, \psi_{Ra\beta} + \psi_{La\alpha}^{\dagger} \, \vec{\sigma}_{\alpha\beta} \, \psi_{La\beta} \right) ,
\tag{2}
$$

where $\vec{\sigma}_{\alpha\beta}$ are the Pauli matrices and $\vec{M}$ is the "exchange field", which is proportional to the magnetization. This is constant in each ferromagnetic lead, i.e. $\vec{M} \parallel \hat{m}_1$ for $x < -L/2$ and $\vec{M} \parallel \hat{m}_2$ for $x > L/2$ and in ordinary paramagnetic leads $\vec{M} = 0$. In this case, the total system corresponding to a nanotube between two ferromagnetic leads is described by the Hamiltonian

$$
H = \int_{|x|>L/2} \mathrm{d}x \; \mathcal{H}_{\mathrm{FM}} + \int_{|x|<L/2} \mathrm{d}x \; \mathcal{H}_{\mathrm{LL}} .
\tag{3}
$$

The total Hamiltonian H can take a form identical to the Hamiltonian in the case of normal metal leads by applying the following transformation to the electron field operators separately in the left and right leads respectively

$$
\begin{aligned}
\psi_{R/L}(x) &\to e^{\pm i/v_{\mathrm{F}} \cdot \int_{-L/2}^{x} \mathrm{d}x' \vec{M}(x') \cdot \vec{\sigma}} \psi_{R/L}(x), \quad x < -\frac{L}{2} \\
\psi_{R/L}(x) &\to e^{\pm i/v_{\mathrm{F}} \cdot \int_{L/2}^{x} \mathrm{d}x' \vec{M}(x') \cdot \vec{\sigma}} \psi_{R/L}(x), \quad x > \frac{L}{2}
\end{aligned}
\tag{4}
$$

This transformation leaves $\mathcal{H}_{\mathrm{LL}}$ invariant and $\mathcal{H}_{\mathrm{FM}}$ transforms into $\mathcal{H}_0$.

We apply the usual bosonization procedure to study this model[22,23]. The four electron modes are associated to four bosonic modes described by the fields $\theta_{a\alpha}$ and their duals $\varphi_{a\alpha}$ via the bosonization transformation

$$
\psi_{R/L a\alpha} = \frac{1}{\sqrt{2\pi\Lambda}} e^{i(\varphi_{a\alpha} \pm \theta_{a\alpha})} ,
\tag{5}
$$

where Λ is a short-distance cutoff. It is convenient to consider the following linear combinations of the fields[25]: $\theta_{i,c/s} = \frac{1}{\sqrt{2}} \left(\theta_{i,\uparrow} \pm \theta_{i,\downarrow} \right)$ and $\theta_{\pm,\mu} = \frac{1}{\sqrt{2}} \left(\theta_{1,\mu} \pm \theta_{2,\mu} \right)$, with $i = 1, 2$ and $\mu = c, s$. This allows us to define the new fields $\theta_1 = \theta_{+c}$, which corresponds to the total charge mode and is the only interacting mode, and $\theta_2 = \theta_{+s}$, $\theta_3 = \theta_{-c}$ and $\theta_4 = \theta_{-s}$; with similar transformations for the φ fields. In terms of these new fields the Luttinger liquid Hamiltonian density (1) is diagonalized

$$
\begin{aligned}
\mathcal{H}_{\mathrm{LL}} = & \frac{v}{2\pi} \left[g \left(\partial_x \varphi_1 \right)^2 + \frac{1}{g} \left(\partial_x \theta_1 \right)^2 \right] \\
& + \sum_{i=2}^{4} \frac{v_{\mathrm{F}}}{2\pi} \left[\left(\partial_x \varphi_i \right)^2 + \left(\partial_x \theta_i \right)^2 \right] ,
\end{aligned}
\tag{6}
$$

where v_{F} is the Fermi velocity, v is the renormalized velocity due to the interactions and g is the Luttinger liquid parameter. In the inhomogeneous model g and v are functions of the position: $g = 1$ and $v = v_{\mathrm{F}}$ in the leads and $g = \sqrt{\frac{v_{\mathrm{F}}}{v_{\mathrm{F}}+8\lambda/\pi}} < 1$ and $v = v_{\mathrm{F}}/g$ in the nanotube.

The contacts between the leads and the nanotube are modeled by weak backscattering at the contact points, the corresponding Hamiltonian density has the form

$$
\begin{aligned}
\mathcal{H}_{\mathrm{bs}} = & \sum_{m=1}^{2} \sum_{a,b=1}^{2} \sum_{\alpha,\beta=\uparrow,\downarrow} \delta(x - x_m) \left[\tilde{u}_m^{ab} \psi_{La\alpha}^\dagger \psi_{Rb\alpha} + \tilde{v}_m^{ab} \psi_{La\alpha}^\dagger \vec{M}_m \cdot \vec{\sigma}_{\alpha\beta} \psi_{Rb\beta} + \mathrm{h.c.} \right] \\
= & \sum_{m,a,b=1}^{2} \sum_{\alpha=\pm 1} \delta(x - x_m) \left\{ \left(u_m^{ab} + \alpha v_m^{ab} M_m^z \right) e^{i \left[\theta_1 + \alpha\theta_2 + (-1)^{a+1}\delta_{ab}(\theta_3 + \alpha\theta_4) + (-1)^{a+1}(1-\delta_{ab})(\varphi_3 + \alpha\varphi_4) \right]} \right. \\
& \left. + v_m^{ab} \left(M_m^x + i\alpha M_m^y \right) e^{i \left[\theta_1 + (-1)^{a+1}\delta_{ab}\theta_3 + (-1)^{a+1}(1-\delta_{ab})\alpha\theta_4 + \alpha\varphi_2 + (-1)^{a+1}(1-\delta_{ab})\varphi_3 + (-1)^{a+1}\delta_{ab}\alpha\varphi_4 \right]} + \mathrm{h.c.} \right\} ,
\end{aligned}
\tag{7}
$$

where m labels the position of the contacts: $x_{1/2} = \mp L/2$ (L is the nanotube length) and u_m^{ab} and v_m^{ab} are constants proportional to the strength of the backscattering, $u_m^{ab} = \tilde{u}_m^{ab}/(2\pi\Lambda)$ and the same for v_m^{ab}. The backscattering terms are restricted by symmetry according to charge conservation and spin rotational symmetry around the axis of magnetization of the ferromagnetic contact. We consider only terms of the form $\psi_R^\dagger \psi_L$ because these are the most relevant in the renormalization group sense (the scaling dimension in real space of these terms is $\Delta = (g+3)/4$, while the scaling dimension of terms of the form $\psi_{R/L}^\dagger \psi_{R/L}$ is $\Delta = 1$). Hence if all scattering terms are weak, these terms will dominate. It is straightforward to extend the present treatment to include the neglected interactions, though we do not attempt this here.

The effect of the magnetization appears only on the backscattering term. In the case of near-perfect contacts to the electrodes, we can treat the backscattering Hamiltonian H_{bs} as a perturbation to the Hamiltonian $H = H_{\mathrm{LL}}$. This procedure is described in section III in the context of the Keldysh formalism that we use in order to account for the effects of the finite bias voltage.

The gate voltage introduces a term in the Hamiltonian density proportional to $\rho V_g = 2/\pi V_g \partial_x \theta_1$, where ρ is the electron density. The constant of proportionality relates the voltage applied at the gate with the voltage felt by the nanotube and therefore depends on the sample. The Hamiltonian density $\mathcal{H} = \mathcal{H}_{\mathrm{LL}} + \mathcal{H}_{V_g}$ becomes

$\mathcal{H} = \mathcal{H}_{\mathrm{LL}}$, after applying the following transformation to the θ_1 field: $\theta_1 \longrightarrow \theta_1 - V_g x$, where we absorbed a constant of proportionality into the definition of V_g for simplicity. This transformation needs to be applied to the total Hamiltonian, including the backscattering term H_{bs}, which means that the gate voltage after this transformation will only contribute to the perturbation Hamiltonian.

The effect of the external magnetic field is introduced via a Zeeman coupling term in the Hamiltonian

$$
H_h = -\vec{h} \cdot \int \mathrm{d}x \left(\psi_{Ra\alpha}^\dagger \vec{\sigma}_{\alpha\beta} \psi_{Ra\beta} + \psi_{La\alpha}^\dagger \vec{\sigma}_{\alpha\beta} \psi_{La\beta} \right) .
\tag{8}
$$

The contribution of the magnetic field can be transfered to the perturbation Hamiltonian H_{bs} using a similar procedure to the one described above for the gate voltage. Taking the z-direction as the direction of the magnetic field, i.e. $\vec{h} = h\hat{z}$, the Zeeman Hamiltonian density becomes $\mathcal{H}_h = -(h/\pi)\partial_x\theta_2$ and applying $\theta_2 \to \theta_2 + Bx$ (with $B = 2h/v_{\mathrm{F}}$), to the Hamiltonian $H = H_{LL} + H_h$, it transforms as $H \to H_{LL}$. The results for non-zero magnetic field are presented in appendix B.

III. THE NON-EQUILIBRIUM TRANSPORT PROBLEM

Due to the finite bias voltage the distribution in this system is not in thermal equilibrium. This non-equilibrium situation is studied using the Keldysh formalism (for a review, see Ref. 29). To define a non-equilibrium initial state, we assume that until some initial time t_0, the system has reached quasi-equilibrium *in the absence of impurity scattering* $u_m^{ab} = v_m^{ab} = 0$. Without impurity scattering, the total number of right- and left-moving carriers, N_R, N_L, are separately conserved, so that a partial equilibrium can be established with well-defined separate chemical potentials for the right and left movers. Hence, the system can be described, up to this time, by a thermal distribution governed by the grand canonical Hamiltonian

$$H_V = H_{\mathrm{LL}} - \mu_1 N_R - \mu_2 N_L \;, \qquad (9)$$

where the chemical potentials in each lead are taken to be $\mu_{1/2} = \mp V/2$ and $N_{R/L} = \int dx\, n_{R/L}$. The right and left moving particle densities are given in the bosonization procedure by $n_{R/L} = \frac{1}{2\pi} \sum_{a\alpha} \partial_x \left(\pm \varphi_{a\alpha} + \theta_{a\alpha} \right)$. Then

$$H_V = H_{\mathrm{LL}} - \int dx\, \frac{2V}{\pi} \, \partial_x \varphi_1 \;. \qquad (10)$$

We emphasize that the appearance of the voltage V in H_V does not represent a physical force on the electrons, but rather parameterizes their non-equilibrium distribution.

After the initial time t_0 the evolution of the system is governed by a different Hamiltonian H, which as deduced in section II is $H = H_{\mathrm{LL}} + H_{\mathrm{bs}}$, with H_{LL} given in (6) and H_{bs} in (7). We expect on physical grounds that introducing localized scattering at the ends of the wire or nanotube reduces the current, but cannot affect the non-equilibrium distribution in the reservoirs. Hence, we believe that the prescription of defining the voltage V from the initial distribution as is done using (9) gives a faithful description of ideal leads. According to this prescription, a physical observable, represented by an operator $\hat{\mathcal{O}}$, is then calculated from

$$\langle \mathcal{O} \rangle = \frac{1}{Z} \mathrm{Tr} \left(e^{-\beta H_V} e^{iHt} \hat{\mathcal{O}} e^{-iHt} \right) \;, \qquad (11)$$

where

$$Z = \mathrm{Tr} \left(e^{-\beta H_V} \right) \;. \qquad (12)$$

The difficulty in evaluating such an expectation value is that, unlike in a conventional equilibrium calculation, the Hamiltonian H_V governing the initial distribution is different from H, which governs the time evolution. Thus such an expectation value cannot be evaluated by equilibrium Green's function techniques.

Instead, we take advantage of the special property of H_V that the voltage couples only to $N_{R/L}$, which are decoupled "zero mode" degrees of freedom. This technique

has been applied a number of times before to related problems[30,31,32], but to our knowledge the details of its derivation have never been published. For completeness, pedagogical value, and to highlight the physical assumptions of the method, we include a thorough derivation in appendix A. The correction to $\langle \mathcal{O} \rangle$ due to the backscattering is given by

$$\langle \delta \mathcal{O} \rangle = \frac{1}{Z_{\mathrm{LL}}} \mathrm{Tr} \left(e^{-\beta H_{\mathrm{LL}}} S^\dagger(t) \hat{\mathcal{O}} S(t) \right) \;, \qquad (13)$$

where

$$S(t) = \mathrm{T} \exp \left[-i \int_0^t dt' \, H_I(t') \right] \qquad (14)$$

is the evolution operator for a system with the time-dependent Hamiltonian $H_I(t')$. Here $H_I(t)$ is the Hamiltonian in the frame co-moving with the ideal current, defined by

$$H_I(t) = e^{it\hat{V}} H e^{-it\hat{V}} = H_{\mathrm{LL}} + [H_{\mathrm{bs}}]_{\theta_1 \to \theta_1 + Vt} \;, \qquad (15)$$

with $\hat{V} = \frac{V}{2}(N_R - N_L)$. Note that (because $[\hat{V}, H_{\mathrm{LL}}] = 0$) all the time dependence in $H_I(t)$ is in the backscattering term, and is hence easy to handle when working perturbatively in H_{bs}.

Eqs. (13-15) provide a reformulation of the transport problem which is particularly convenient for a perturbative treatment of the backscattering. Note that – because the voltage V appears only within H_{bs} – a direct expansion of Eq. (13) in H_{bs} will involve *equilibrium* real-time propagators calculated with respect to H_{LL}. We develop this perturbation theory using the Keldysh path integral formulation. This involves the usual Trotterization of the two evolution operators $S^\dagger, S$ in Eq. (13) using coherent-state fields denoted θ^+, φ^+ for S ("forward branch") and θ^-, φ^- ("backward branch") for $S^\dagger$. Further noting that H_{LL} is quadratic and H_{bs} acts only at the ends of the nanotube/wire, the fields away from $x = \pm L/2$ can be integrated out to obtain the Keldysh integral

$$\langle \delta \mathcal{O} \rangle = \int \mathcal{D}[\theta^\pm(t) \varphi^\pm(t)] \mathcal{O}_K e^{iS_0 - i \int dt H_{\mathrm{pert}}(t)} \;, \qquad (16)$$

with

$$H_{\mathrm{pert}} = H_{\mathrm{bs}}[\varphi_i^+, \theta_i^+ + \delta_{i1} Vt] - H_{\mathrm{bs}}[\varphi_i^-, \theta_i^- + \delta_{i1} Vt] \;. \qquad (17)$$

Here $\mathcal{O}_K$ is an appropriate Keldysh representation of the operator $\mathcal{O}$, which can be chosen as usual from fields lying on either the forward or backward moving branch, or any linear combination thereof – see below for convenient choices. The quadratic action S_0 is a functional of $\theta^\pm(t), \varphi^\pm(t)$, which can be determined from the fact that it must reproduce the *equilibrium* correlation and response functions for these fields. Indeed, we do not require an explicit expression for S_0, but instead give the response and correlation functions, defined by

$$C^\theta(x,t;x',t') = \langle \theta(x,t)\theta(x',t') \rangle = \tfrac{1}{2} \langle \{ \hat{\theta}(x,t), \hat{\theta}(x',t') \} \rangle \;,$$
$$R^\theta(x,t;x',t') = \langle \theta(x,t)\tilde{\theta}(x',t') \rangle =$$
$$= -i\Theta(t-t') \langle [\hat{\theta}(x,t), \hat{\theta}(x',t')] \rangle \;, \qquad (18)$$

where we have applied the standard Keldysh rotation to the fields $\theta^\pm = \theta \pm \frac{i}{2}\tilde{\theta}$. By construction $\langle\tilde{\theta}(x,t)\tilde{\theta}(x',t')\rangle = 0$. The Green's functions involving the φ fields are defined in a similar way, replacing θ by φ in the above equations. There are also Green's functions that involve both θ and φ, these are defined by

$$C^{\theta\varphi}(x,t;x',t') = \langle\theta(x,t)\varphi(x',t')\rangle = \tfrac{1}{2}\langle\{\hat{\theta}(x,t),\hat{\varphi}(x',t')\}\rangle$$
$$R^{\theta\varphi}(x,t;x',t') = \langle\theta(x,t)\tilde{\varphi}(x',t')\rangle =$$
$$= -i\Theta(t-t')\langle[\hat{\theta}(x,t),\hat{\varphi}(x',t')]\rangle , \quad (19)$$

and similar definitions for $C^{\varphi\theta}$ and $R^{\varphi\theta}$. Again, by construction $\langle\tilde{\theta}(x,t)\tilde{\varphi}(x',t')\rangle = \langle\tilde{\varphi}(x,t)\tilde{\theta}(x',t')\rangle = 0$.

Using the above procedure we obtain (up to additive constants that will not contribute to the final result) the Green's functions for the θ_1 fields:

$$R_{11}^{\theta I}(t) = -\frac{\pi}{2}(1-\alpha)\left[\Theta(t) + \frac{1+\alpha}{\alpha}\sum_{k\geq1}\alpha^{2k}\Theta(t-2kt_v)\right]$$

$$R_{12}^{\theta I}(t) = -\frac{\pi}{2}(1-\alpha^2)\sum_{k\geq0}\alpha^{2k}\Theta(t-(2k+1)t_v) ,$$

$$C_{11}^{\theta I}(t) = -\frac{1-\alpha}{4}\left[\log t^2 + \right.$$
$$\left. + \frac{1+\alpha}{\alpha}\sum_{k\geq1}\alpha^{2k}\log\left|t^2-(2kt_v)^2\right|\right] ,$$

$$C_{12}^{\theta I}(t) = -\frac{1-\alpha^2}{4}\sum_{k\geq0}\alpha^{2k}\log\left|t^2-[(2k+1)t_v]^2\right| ,$$
$$(20)$$

where the subscripts label the position of the contacts $x_{1,2}$ (e.g. $C_{ab}(t) = C(x_a,t;x_b,0)$) and

$$\alpha = \frac{1-g}{1+g} \quad\text{and}\quad t_v = \frac{L}{v} . \quad (21)$$

We also need the Green's functions for the non-interacting modes $\theta_{2,3,4}$, R^F and C^F. These are obtained from (20) by taking $\alpha = 0$ and replacing t_v by $t_F = L/v_F$,

$$R_{11}^F(t) = -\frac{\pi}{2}\Theta(t) ,$$
$$R_{12}^F(t) = -\frac{\pi}{2}\Theta(t-t_F) ,$$
$$C_{11}^F(t) = -\frac{1}{4}\log t^2 ,$$
$$C_{12}^F(t) = -\frac{1}{4}\log\left|t^2-t_F^2\right| . \quad (22)$$

The Green's functions for the φ fields can be obtained from those for the θ fields given in (20), by replacing g by $1/g$, i.e. by replacing α by $-\alpha$. On the other hand, the only φ Green's functions that contribute to the transport properties studied in the following sessions are those

that correspond to the non-interacting modes $\varphi_{2,3,4}$, and therefore they are identical to the functions given in (22).

In order to compute the spin transport properties in section V, we also need the following functions for the θ_2 and φ_2 fields

$$R^{\theta_2\varphi_2}(x,t) = \text{sign}(x)\frac{\pi}{2}\,\Theta(t)\,\Theta(|x|-v_F t) ,$$
$$C^{\theta_2\varphi_2}(x,t) = -\frac{1}{4}\,\log\left|\frac{v_F t-x}{v_F t+x}\right| , \quad (23)$$

$C^{\varphi_2\theta_2}(x,t) = C^{\theta_2\varphi_2}(x,t)$ and $R^{\varphi_2\theta_2}(x,t) = R^{\theta_2\varphi_2}(x,t)$.

IV. THE DIFFERENTIAL CONDUCTANCE

In this section we study the charge transport properties of 1D electron systems and how these are affected by the magnetization of the leads and, more importantly, the presence of the strong Coulomb interactions.

We use the procedure described in sections II and III to calculate the differential conductance for these systems. This is obtained from the expectation value of the current in a nanotube, i.e. a four mode 1D electron system with the Hamiltonian given in (6), as

$$I = \sum_{a\alpha}\langle\psi_{Ra\alpha}^\dagger\psi_{Ra\alpha} - \psi_{La\alpha}^\dagger\psi_{La\alpha}\rangle = \frac{2}{\pi}\langle\partial_t\theta_1\rangle . \quad (24)$$

After a lengthy but straightforward calculation we obtain that the differential conductance $G = \partial I/\partial V$ to second order in perturbation theory is given by

$$G = \frac{2}{\pi}\left\{1 + \sum_m U_m\int\!dt\,t\,e^{\boldsymbol{C}_{1m}(t)}\sin\left[\frac{1}{2}\boldsymbol{R}_{1m}(t)\right]\cos(Vt)\right\}$$
$$(25)$$

with

$$U_1 = \sum_{mab}\left[\left(u_m^{ab}\right)^2 + \left(v_m^{ab}\right)^2\vec{M}_m^2\right] , \quad (26)$$
$$U_2 = 2\cos(V_g L)\sum_{ab}\left[u_1^{ab}u_2^{ab} + v_1^{ab}v_2^{ab}\vec{M}_1\cdot\vec{M}_2\right] ,$$

and

$$\boldsymbol{C}_{ab}(t) = C_{ab}^{\theta I}(t) + 3C_{ab}^F(t) , \quad (27)$$

and similarly for $\boldsymbol{R}_{ab}(t)$. For a quantum wire (i.e. a single-channel electron system) these are replaced by $\boldsymbol{C}_{ab}(t) = 2\left(C_{ab}^{\theta I}(t) + C_{ab}^F(t)\right)$ and the global normalization is divided by a factor of two (since the quantum wire has two modes instead of four).

Eqs. (25) and (26) are valid for zero external magnetic field, which is the case considered in this section, the equations for non-zero magnetic field are presented in appendix B.

Equation (25) can be easily generalized to arbitrary order in perturbation theory, but the time integrals need

to be computed numerically. We present the calculated conductance to second order for three different physical models in Fig. 3. This models correspond to (a) a nanotube with non-interacting electrons, i.e. taking $g = 1$, (b) a quantum wire with $g = 0.5$ and (c) a nanotube with $g = 0.25$, which is a physically relevant value for single-walled carbon nanotubes[16,17,18,19,25]. The effect of the interactions is visible in the dependence of the conductance with bias voltage, at constant gate voltage.

The conductance is a quasi-periodic function of the bias voltage. At $V_g = 0$, for the non-interacting case, see Fig. 3.(a), this dependence is a cosine function with period $2\pi/t_F$. For a quantum wire, Fig. 3.(b), there are clearly two different "periods" in the oscillations, these are related to the two time scales $t_F = L/v_{\rm F}$ and $t_v = gt_F = L/v$. The existence of these two different time scales is due to the two bosonic excitations in this system: The spin excitation with velocity $v_{\rm F}$ and the charge excitation with velocity v, and is therefore an effect of spin charge separation. The same effect appears in Fig. 3.(c), but since for the nanotube there are three non-interacting modes with velocity $v_{\rm F}$ and only one mode, the total charge, with velocity v, it is less visible than in the previous example. The most visible effect of the interactions in the nanotube, is the enhancement of the amplitude in the conductance around $V = 0$. This effect is observable in the experimental data presented in Ref. 14.

The calculated conductance at $V_g L = \pi/2$ as a function of the bias voltage for a nanotube with different interaction strengths corresponding to $g = 0.25$, 0.5 and 1, is presented in Fig. 4. It can be seen using Eqs. (25) and (26) that the conductance for this value of the gate voltage only depends on the Green's functions C_{11} and R_{11}, which depends only on t_v. As a result, we can clearly see in Fig. 4 that the period of the oscillations is π/t_v, and therefore depends strongly on the interaction strength. The amplitude of this oscillations is very small except for the first oscillation, which is enough to identify this effect.

As for the dependence with the gate voltage, the conductance is a periodic function, which is modulated by $\vec{M}_1 \cdot \vec{M}_2$, and this is the main effect of the magnetization in the leads on the conductance. In particular if $\sum u_1^{ab} u_2^{ab} \leq \sum v_1^{ab} v_2^{ab}$, there is an angle between the two magnetizations for which U_2 vanishes for any value of the gate voltage, in this case the conductance is given also in Fig. 4.

V.   SPIN TRANSPORT

In this section we study spin transport properties, i.e. the spin density in the nanotube and the spin current generated by the magnetization in the leads.

The spin density expectation value in the nanotube, calculated using bosonization and the Keldysh perturbation formalism as described in sections II and III, is given by

$$\vec{S} = \frac{1}{2} \sum_{a\alpha\beta} \langle \psi_{R a \alpha}^\dagger \, \vec{\sigma}_{\alpha\beta} \, \psi_{R a \beta} + \psi_{L a \alpha}^\dagger \, \vec{\sigma}_{\alpha\beta} \, \psi_{L a \beta} \rangle \ . \quad (28)$$

For zero magnetic field, it is technically simplest to calculate S^z from the bosonized form

$$S^z = \frac{1}{\pi} \langle \partial_x \theta_2 \rangle \quad (29)$$

and then obtain the other two components by rotational invariance. For non-zero magnetic field the calculation as well as the final results are much more involved, therefore and for the sake of clarity we only present the results in appendix B.

The result is

$$\vec{S} = -\frac{1}{v_{\rm F}} \left(\vec{u}_1 \int dt\, e^{C_{11}(t)} \sin\left[\frac{1}{2} R_{11}(t)\right] \sin(Vt) \right.$$
$$+ \sin(V_g L) \left\{ \vec{u}_2 \int dt\, e^{C_{12}(t)} \sin\left[\frac{1}{2} R_{12}(t)\right] \sin(Vt) \right.$$
$$\left. \left. + \vec{u}_3 \int dt\, e^{C_{12}(t)} \sin\left[\frac{1}{2} R_{12}(t)\right] \cos(Vt) \right\} \right) \ , \quad (30)$$

with

$$\vec{u}_1 = \sum_{ab} \left(u_1^{ab} v_1^{ab} \vec{M}_1 - u_2^{ab} v_2^{ab} \vec{M}_2 \right) \ ,$$
$$\vec{u}_2 = \sum_{ab} v_1^{ab} v_2^{ab} \vec{M}_1 \times \vec{M}_2 \ ,$$
$$\vec{u}_3 = \sum_{ab} \left(u_1^{ab} v_2^{ab} \vec{M}_2 + u_2^{ab} v_1^{ab} \vec{M}_1 \right) \ . \quad (31)$$

Notice that the spin density does not depend on the position in the nanotube, hence the total spin is $L\vec{S}$.

The first term, proportional to $\vec{u}_1$, is the known non-equilibrium spin accumulation effect[1,2,3,4,5,6]. It is maximum for $\vec{M}_1 = -\vec{M}_2$, when, in the case of identical contacts, the other terms vanish. This term does not couple two backscatterers, is independent of the gate voltage, and is an increasing function of the bias voltage. It is depicted in Fig. 5(a), since it is the only term term that corresponds to the component of the spin in the direction of $\vec{M}_1$ at $V_g = 0$. The second term corresponds to the component of the spin perpendicular to the plane of the magnetizations and is depicted in Fig. 5(c), as function of the bias and gate voltages. The third term is the only one that survives in equilibrium, i.e. at zero bias, it is due to the fact that the backscattering strengths depend on the spins of the incoming and outgoing electron relative to the direction of the magnetizations. It is maximum for $\vec{M}_1 = \vec{M}_2$, when again for identical contacts the other terms vanish. This is depicted in Fig. 5(b), at $\theta = 0, 2\pi$. These terms that couple the two backscatterers, and hence depend on the gate voltage, vary with bias voltage in a manner approximately described by a sum of two periodic functions, with "periods" given by
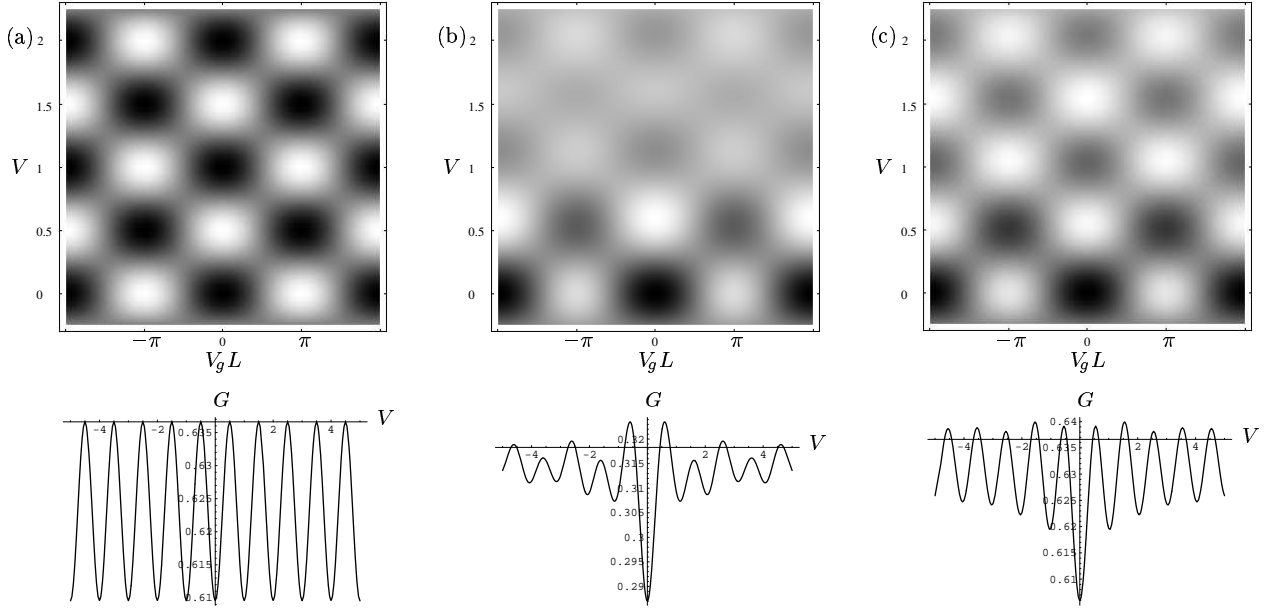
FIG. 3: Calculated conductance for identical contacts and $\vec{M}_1 = \vec{M}_2$ for (a) a free electron model, i.e. a nanotube with $g = 1$; (b) a quantum wire, i.e. a LL with two modes: spin and charge, with $g = 0.5$; and (c) a nanotube with $g = 0.25$, as a function of bias V and gate V_g voltages (top) and as a function of the bias voltage V at constant gate voltage $V_g = 0$ (bottom). As can be seen, the effect of the interactions is quite appreciable, in particular with the dependence in bias voltage at $V_g = 0$. The "period" of these oscillations is given by $2\pi/t_F$ ($t_F = 2\pi$ in these figures), in agreement with Ref. 14, but in (b) and (c) there is another quasi-periodic component in these oscillations, with period given by $2\pi/t_v$, the presence of these two time scales, t_F and t_v, is a direct result of spin charge separation.

$2\pi/t_F$ and $2\pi/t_v$, as discussed in the previous section for the conductance.

The spin current

$$\vec{J}_s = \frac{v_F}{2} \sum_{a\alpha\beta} \langle \psi^\dagger_{Ra\alpha} \vec{\sigma}_{\alpha\beta} \psi_{Ra\beta} - \psi^\dagger_{La\alpha} \vec{\sigma}_{\alpha\beta} \psi_{La\beta} \rangle \quad (32)$$

is as the spin density calculated from the J_s^z component in its bosonized form (again see result for non-zero mag-

netic field in appendix B)

$$J_s^z = \frac{1}{\pi} \langle \partial_t \theta_2 \rangle . \quad (33)$$

It is not well-defined at the contact points because the backscattering term in the Hamiltonian (7) does not conserve spin, and therefore it has different expressions in the nanotube and the leads.

The spin current in the left $(+)$ and right $(-)$ leads is given by

$$\vec{J}_s = \vec{u}_4 \int dt\, e^{C_{11}(t)} \sin\left[\frac{1}{2}R_{11}(t)\right] \sin(Vt)$$
$$+ [\pm \sin(V_gL)\, \vec{u}_2 + \cos(V_gL)\, \vec{u}_3]$$
$$\times \int dt\, e^{C_{12}(t)} \sin\left[\frac{1}{2}R_{12}(t)\right] \sin(Vt) \quad (34)$$

and in the nanotube by:

$$\vec{J}_s = \vec{u}_4 \int dt\, e^{C_{11}(t)} \sin\left[\frac{1}{2}R_{11}(t)\right] \sin(Vt) \quad (35)$$
$$+ \cos(V_gL) \left\{ \vec{u}_2 \int dt\, e^{C_{12}(t)} \sin\left[\frac{1}{2}R_{12}(t)\right] \cos(Vt) \right.$$
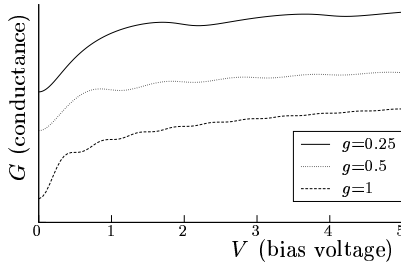$$\left. + \vec{u}_3 \int dt\, e^{C_{12}(t)} \sin\left[\frac{1}{2}R_{12}(t)\right] \sin(Vt) \right\} .$$

FIG. 4: At constant gate voltage: $V_gL = \pi/2$, the period of oscillations is π/gt_L, i.e. depends strongly on the interaction strength. In order for this effect to be clearly visible, we scaled and shifted the functions differently, therefore the values of the G axes are not meaningful.
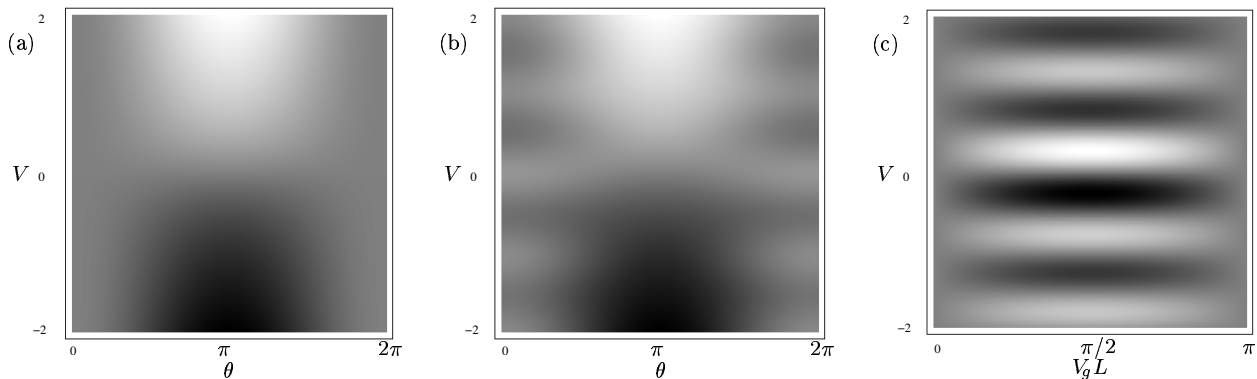
FIG. 5: Calculated spin for a nanotube with $g = 0.25$, the component of the spin in the direction of the magnetization $\vec{M}_1$ as function of the angle between the two magnetizations θ and the bias voltage V, at constant gate voltage (a) $V_g = 0$ and (b) $V_g = \pi/2$; and (c) the component of the spin perpendicular to the plane formed by the two magnetizations as a function of the gate and bias voltages.

with $\vec{u}_2$ and $\vec{u}_3$ defined in (31) and

$$\vec{u}_4 = \sum_{mab} u_m^{ab} v_m^{ab} \vec{M}_m . \qquad (36)$$

Similarly to the results for the spin discussed above, the first term, which only involves one backscatterer and is independent of the gate voltage, corresponds to the usual spin injection effect. It is an increasing function of the gate voltage and is maximum for $\vec{M}_1 = \vec{M}_2$. This can be seen in Fig. 6(b), since it is the only term that does not vanish in the direction of $\vec{M}_1$ at $V_g L = \pi/2$. At $V_g = 0$, the terms proportional to $\vec{u}_1$ and $\vec{u}_3$ contribute equally to the component of the current in the direction of $\vec{M}_1$, the result for this case is presented in Fig. 6(a). The second term, proportional to $\vec{M}_1 \times \vec{M}_2$ corresponds to an exchange interaction between the magnetizations of the leads, mediated by the nanotube. It has opposite signs in the two leads and it is shown in Fig. 6(c).

VI. CONCLUSIONS

We studied the charge and spin transport properties of 1D systems, e.g. quantum wires and carbon nanotubes, focusing on the latter. We considered the case of nearly perfect ohmic contact between the 1D system and the electrodes and included the strong Coulomb interaction via a Luttinger liquid model. We found important effects on the transport properties of these systems that are due to the Coulomb interactions. These appear in the dependence with bias voltage. In particular, the conductance is enhanced at low bias voltage, furthermore it is an oscillatory function where we can distinguish two quasi-periodic components, with periods that are related to the two velocities of the excitations of a Luttinger liquid, v and v_F. This effect is therefore a direct consequence of spin and charge separation. It is clearly visible in single band quantum wires. In nanotubes, the amplitude of

the higher period component is reduced by the presence of three (as opposed to one) neutral modes. Still, we can find evidence of the two velocities v and v_F by comparing the dependence of the conductance with bias voltage for two different gate voltages ($V_g L = 0$ and $\pi/2$). It is perhaps worth noting that, for the case of non-magnetic leads with symmetric contacts, the conductance formula involves only two unknown parameters: the overall amplitude of the backscattered current, and the Luttinger parameter g, both of which can be simply estimated. Nevertheless, a non-trivial functional dependence upon bias voltage is predicted.

The spin and spin current have one component in the plane of the magnetization that does not couple the two leads and is therefore independent of the gate voltage. This term should be understood as arising from incoherent spin injection at each contact. It is a monotonic function of the bias voltage, and corresponds to the known spin accumulation (for the spin) and spin injection (for the spin current) effects. The other components that couple the two leads, and therefore depend on the gate voltage, are backscattering processes occurring with coherence between the two contacts. These oscillate with the bias voltage, in a manner approximately described as a sum of two periodic components, with periods related to the two velocities of the excitation of the Luttinger liquid. The amplitude of the higher-period component is largest in a single-channel quantum wire, and somewhat suppressed in nanotubes by the sub-band degeneracy.
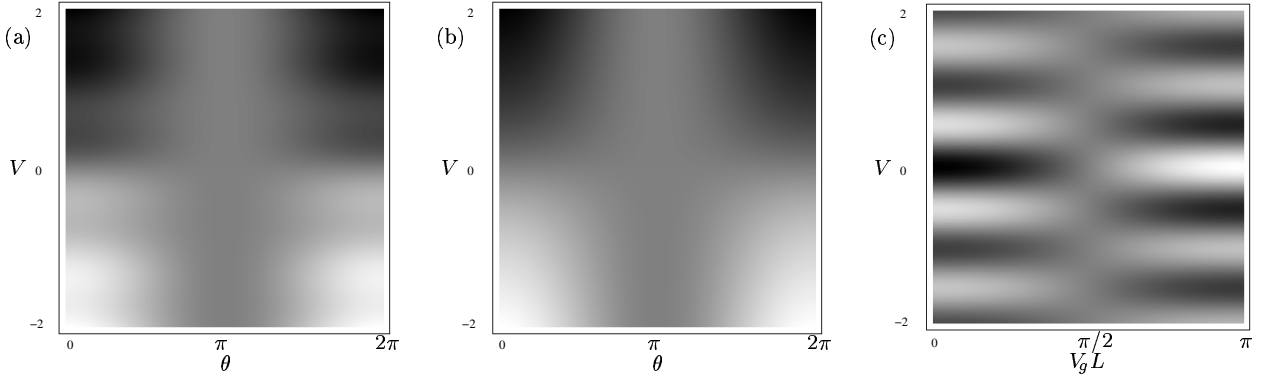
FIG. 6: Calculated spin current for a nanotube with $g = 0.25$: the component of the spin current in the direction of the magnetization $\vec{M}_1$ as function of the angle between the two magnetizations θ and the bias voltage V, at constant gate voltage (a) $V_g = 0$ and (b) $V_g = \pi/2$; and (c) the component of the spin current perpendicular to the plane formed by the two magnetizations as a function of the gate and bias voltages (this figure corresponds to the spin current in the nanotube, in the leads this component of the spin current is identical to Fig. 5.(c)).

APPENDIX A: DERIVATION OF EQ. (13)

In this appendix, we derive Eq. (13). In particular, we consider a large periodic system of size L, where ultimately $\mathsf{L} \to \infty$. We define the right/left-moving combinations

$$\phi_{iR/L} = \varphi_i \pm \theta_i . \tag{A1}$$

In the system of size L we can decompose into finite wavevector and "zero mode" components. In particular, for the total charge fields, we define

$$\phi_{1R}(x) = \tilde{\phi}_{1R}(x) + \frac{2\pi N_R x}{\mathsf{L}} + \Phi_R , \tag{A2}$$

$$\phi_{1L}(x) = \tilde{\phi}_{1L}(x) - \frac{2\pi N_L x}{\mathsf{L}} + \Phi_L , \tag{A3}$$

where $\tilde{\phi}_{1R/L}(x)$ contains the non-zero momentum modes of the $\phi_{1R/L}$ fields. With these definitions, the zero-mode variables form two canonically conjugate pairs:

$$[N_R, \Phi_R] = [N_L, \Phi_L] = i , \tag{A4}$$
$$[N_R, \Phi_L] = [N_L, \Phi_R] = [N_R, N_L] = [\Phi_R, \Phi_L] = 0 .$$

Moreover, $N_{R/L}, \Phi_{R/L}$ commute with $\tilde{\phi}_{1R/L}(x)$ and all fields associated with channels $2, 3, 4$.

Since the interactions which transform the system from a Fermi liquid into a Luttinger liquid (Eq. (1)) exist only for $|x| < L/2$, they do not affect the zero-mode terms in the Hamiltonian. Hence one may separate

$$H_V = \tilde{H}_{\mathrm{LL}} + \frac{\pi v_{\mathrm{F}}}{\mathsf{L}} \left(N_R^2 + N_L^2 \right) - \frac{V}{2} \left(N_R - N_L \right) , \tag{A5}$$

where $\tilde{H}_{\mathrm{LL}}$ is the Luttinger liquid Hamiltonian, Eq. (6), with the zero-mode terms subtracted, i.e. with $\varphi_1 \to \tilde{\varphi}_1$

and $\theta_1 \to \tilde{\theta}_1$. We then see, using the independence of the zero mode variables, that the unitary operator

$$U_V = e^{i\frac{V\mathsf{L}}{4\pi v_{\mathrm{F}}}(\Phi_R - \Phi_L)} , \tag{A6}$$

generates the following transformation $N_{R/L} \to N_{R/L} \pm V\mathsf{L}/(4\pi v_{\mathrm{F}})$, hence

$$e^{-\beta H_V} = e^{-\mathcal{C}} U_V e^{-\beta H_{\mathrm{LL}}} U_V^\dagger , \tag{A7}$$

where $\mathcal{C} = \beta \mathsf{L}/(8\pi v_{\mathrm{F}})$ is an unimportant constant. Inserting this into Eqs. (11-12), one obtains

$$\langle \mathcal{O} \rangle = \frac{1}{Z_{\mathrm{LL}}} \mathrm{Tr} \left(e^{-\beta H_{\mathrm{LL}}} e^{i(H+\hat{V})t} \left(U_V^\dagger \hat{\mathcal{O}} U_V \right) e^{-i(H+\hat{V})t} \right) , \tag{A8}$$

with

$$Z_{\mathrm{LL}} = \mathrm{Tr} \left(e^{-\beta H_{\mathrm{LL}}} \right) \tag{A9}$$

and

$$\hat{V} = \frac{V}{2} (N_R - N_L) . \tag{A10}$$

For the operators of interest,

$$U_V^\dagger \hat{I} U_V = I_0 + \hat{I} , \tag{A11}$$
$$U_V^\dagger \vec{S} U_V = \vec{S} , \tag{A12}$$
$$U_V^\dagger \vec{J}_s U_V = \vec{J}_s , \tag{A13}$$

where $I_0 = 4(e^2/h)V = (2/\pi)V$ is the current which would flow in an ideal nanotube in the absence of backscattering. Defining $\delta\mathcal{O} = \mathcal{O} - \mathcal{O}_0$, with $\mathcal{O}_0 = I_0$ for $\mathcal{O} = \hat{I}$ and $\mathcal{O}_0 = 0$ for $\mathcal{O} = \vec{S}, \vec{J}_s$, one has then

$$\langle \delta\mathcal{O} \rangle = \frac{1}{Z_{\mathrm{LL}}} \mathrm{Tr} \left(e^{-\beta H_{\mathrm{LL}}} e^{i(H+\hat{V})t} \hat{\mathcal{O}} e^{-i(H+\hat{V})t} \right) . \tag{A14}$$

We then apply the formula

$$e^{-it(H+\hat{V})} = e^{-it\hat{V}} \, \mathrm{T} \exp \left[-i \int_0^t \mathrm{d}t' \, H_I(t') \right] , \tag{A15}$$

to arrive at Eqs. (13) ff. given in the main text.

APPENDIX B: DIFFERENTIAL CONDUCTANCE, SPIN AND SPIN CURRENT AT NON-ZERO MAGNETIC FIELD

The differential conductance including the magnetic field is still given by Eqs. (25) and (26) with only the following change in U_2

$$
\begin{aligned}
U_2 =& 2\cos(V_g L)\sum_{ab}\left\{u_1^{ab}u_2^{ab} + v_1^{ab}v_2^{ab}\left[\vec{M}_1\cdot\vec{M}_2 + (\vec{M}_1\cdot\hat{h})(\vec{M}_2\cdot\hat{h})\left(\cos BL - 1\right)\right]\right\} \\
&+ \sin(BL)\sin(V_g L)\sum_{ab}\left[u_1^{ab}v_2^{ab}(\vec{M}_2\cdot\hat{h}) + u_2^{ab}v_1^{ab}(M_1\cdot\hat{h})\right] ,
\end{aligned}
\tag{B1}
$$

where $\hat{h} = \vec{h}/h$.

The total spin of the nanotube is

$$
\begin{aligned}
\vec{S} =& \frac{1}{\pi}\hat{h}BL - \frac{1}{v_{\mathrm{F}}}\sum_{ab}\Bigg(\Bigg\{\left(u_1^{ab}v_1^{ab}\vec{M}_1 - u_2^{ab}v_2^{ab}\vec{M}_2\right)\frac{1}{B}\sin BL + \left(u_1^{ab}v_1^{ab}(\vec{M}_1\cdot\hat{h})\hat{h} - u_2^{ab}v_2^{ab}(\vec{M}_2\cdot\hat{h})\hat{h}\right)\left(L - \frac{1}{B}\sin BL\right) \\
&+ \left(u_1^{ab}v_1^{ab}(\vec{M}_1\times\hat{h}) - u_2^{ab}v_2^{ab}(\vec{M}_2\times\hat{h})\right)\frac{1}{B}\left(1 - \cos BL\right)\Bigg\}\int_t e^{\boldsymbol{C}_{11}}\sin\left(\tfrac{1}{2}\boldsymbol{R}_{11}\right)\sin(Vt) \\
&+ \Bigg\{\left[\left(u_1^{ab}v_2^{ab}\vec{M}_2 + u_2^{ab}v_1^{ab}\vec{M}_1\right)\frac{1}{B}\sin BL + \left(u_1^{ab}v_2^{ab}(\vec{M}_2\cdot\hat{h})\hat{h} + u_2^{ab}v_1^{ab}(\vec{M}_1\cdot\hat{h})\hat{h}\right)\left(L\cos BL - \frac{1}{B}\sin BL\right)\right]\sin V_g L \\
&- u_1^{ab}u_2^{ab}\hat{h}L\sin BL\cos V_g L - v_1^{ab}v_2^{ab}\left[\left((\vec{M}_1\cdot\hat{h})\vec{M}_2 + (\vec{M}_2\cdot\hat{h})\vec{M}_1\right)\frac{1}{B}\left(1 - \cos BL\right)\right. \\
&\left.+ (\vec{M}_1\cdot\hat{h})(\vec{M}_2\cdot\hat{h})\hat{h}\left(L\sin BL - \frac{2}{B}\left(1 - \cos BL\right)\right)\right]\cos V_g L\Bigg\}\int_t e^{\boldsymbol{C}_{12}}\sin\left(\tfrac{1}{2}\boldsymbol{R}_{12}\right)\cos(Vt) \\
&+ \Bigg\{\left(u_1^{ab}v_2^{ab}(\vec{M}_2\times\hat{h}) - u_2^{ab}v_1^{ab}(\vec{M}_1\times\hat{h})\right)\frac{1}{B}\left(1 - \cos BL\right)\cos V_g L + v_1^{ab}v_2^{ab}\left[\left((\vec{M}_1\cdot\hat{h})(\vec{M}_2\times\hat{h}) - (\vec{M}_2\cdot\hat{h})(\vec{M}_1\times\hat{h})\right)\right. \\
&\left.\times\left(L - \frac{1}{B}\sin BL\right) + \vec{M}_1\times\vec{M}_2 L\right]\sin V_g L\Bigg\}\int_t e^{\boldsymbol{C}_{12}}\sin\left(\tfrac{1}{2}\boldsymbol{R}_{12}\right)\sin(Vt)\Bigg) .
\end{aligned}
\tag{B2}
$$

The spin current in the nanotube (Eq. B3) and the leads (Eq. B4) is

$$
\begin{aligned}
\vec{J}_s = \sum_{ab} & \left\{ u_1^{ab} v_1^{ab} \vec{M}_1 \cos B(x-x_1) + u_2^{ab} v_2^{ab} \vec{M}_2 \cos B(x-x_2) \right. \\
& + u_1^{ab} v_1^{ab} (\vec{M}_1 \cdot \hat{h}) \hat{h} \left[1 - \cos B(x-x_1)\right] + u_2^{ab} v_2^{ab} (\vec{M}_2 \cdot \hat{h}) \hat{h} \left[1 - \cos B(x-x_2)\right] \\
& \left. + u_1^{ab} v_1^{ab} (\vec{M}_1 \times \hat{h}) \sin B(x-x_1) - u_2^{ab} v_2^{ab} (\vec{M}_2 \times \hat{h}) \sin B(x-x_2) \right\} \int_t e^{\boldsymbol{C}_{11}} \sin\left(\tfrac{1}{2}\boldsymbol{R}_{11}\right) \sin(Vt) \\
+ \sum_{ab} & \left\{ \left[u_1^{ab} v_2^{ab} (\vec{M}_2 \cdot \hat{h}) \hat{h} \left[\cos BL - \cos B(x-x_1)\right] + u_2^{ab} v_1^{ab} (\vec{M}_1 \cdot \hat{h}) \hat{h} \left[\cos BL - \cos B(x-x_2)\right] \right. \right. \\
& \left. + u_1^{ab} v_2^{ab} \vec{M}_2 \cos B(x-x_1) + u_2^{ab} v_1^{ab} \vec{M}_1 \cos B(x-x_2) \right] \cos V_g L \\
& + v_1^{ab} v_2^{ab} \left[(\vec{M}_1 \cdot \hat{h})(\vec{M}_2 \cdot \hat{h}) \hat{h} \left[\sin BL - \sin B(x-x_1) + \sin B(x-x_2)\right] \right. \\
& \quad + (\vec{M}_1 \cdot \hat{h})\vec{M}_2 \sin B(x-x_1) - (\vec{M}_2 \cdot \hat{h})\vec{M}_1 \sin B(x-x_2) \\
& \left. \left. \quad + u_1^{ab} u_2^{ab} \hat{h} \sin BL \right] \sin V_g L \right\} \int_t e^{\boldsymbol{C}_{12}} \sin\left(\tfrac{1}{2}\boldsymbol{R}_{12}\right) \sin(Vt) \\
+ \sum_{ab} & \left\{ \left[u_1^{ab} v_2^{ab} (\vec{M}_2 \times \hat{h}) \sin B(x-x_1) - u_2^{ab} v_1^{ab} (\vec{M}_1 \times \hat{h}) \sin B(x-x_2) \right] \sin V_g L \right. \\
& - v_1^{ab} v_2^{ab} \left[(\vec{M}_1 \cdot \hat{h})(\vec{M}_2 \times \hat{h}) \left[1 - \cos B(x-x_1)\right] - (\vec{M}_2 \cdot \hat{h})(\vec{M}_1 \times \hat{h}) \left[1 - \cos B(x-x_2)\right] \right. \\
& \left. \left. + \vec{M}_1 \times \vec{M}_2 \right] \cos V_g L \right\} \int_t e^{\boldsymbol{C}_{12}} \sin\left(\tfrac{1}{2}\boldsymbol{R}_{12}\right) \cos(Vt) \, ,
\end{aligned}
\tag{B3}
$$

$$
\begin{aligned}
\vec{J}_s = \sum_{ab} & \left\{ u_1^{ab} v_1^{ab} \vec{M}_1 \cos B(x-x_1) + u_2^{ab} v_2^{ab} \vec{M}_2 \cos B(x-x_2) \right. \\
& + u_1^{ab} v_1^{ab} (\vec{M}_1 \cdot \hat{h}) \hat{h} \left[1 - \cos B(x-x_1)\right] + u_2^{ab} v_2^{ab} (\vec{M}_2 \cdot \hat{h}) \hat{h} \left[1 - \cos B(x-x_2)\right] \\
& \left. \mp \left[u_1^{ab} v_1^{ab} (\vec{M}_1 \times \hat{h}) \sin B(x-x_1) + u_2^{ab} v_2^{ab} (\vec{M}_2 \times \hat{h}) \sin B(x-x_2) \right] \right\} \int_t e^{\boldsymbol{C}_{11}} \sin\left(\tfrac{1}{2}\boldsymbol{R}_{11}\right) \sin(Vt) \\
+ \sum_{ab} & \left\{ \left[u_1^{ab} v_2^{ab} (\vec{M}_2 \cdot \hat{h}) \hat{h} \left[\cos BL - \cos B(x-x_1)\right] + u_2^{ab} v_1^{ab} (\vec{M}_1 \cdot \hat{h}) \hat{h} \left[\cos BL - \cos B(x-x_2)\right] \right. \right. \\
& \left. + u_1^{ab} v_2^{ab} \vec{M}_2 \cos B(x-x_1) + u_2^{ab} v_1^{ab} \vec{M}_1 \cos B(x-x_2) \right] \cos V_g L \\
& + v_1^{ab} v_2^{ab} \left[(\vec{M}_1 \cdot \hat{h})(\vec{M}_2 \cdot \hat{h}) \hat{h} \left[\sin BL - \sin B(x-x_1) + \sin B(x-x_2)\right] \right. \\
& \left. \quad + (\vec{M}_1 \cdot \hat{h})\vec{M}_2 \sin B(x-x_1) - (\vec{M}_2 \cdot \hat{h})\vec{M}_1 \sin B(x-x_2) \right] \sin V_g L \\
& \mp \left[u_1^{ab} v_2^{ab} (\vec{M}_2 \times \hat{h}) \sin B(x-x_1) + u_2^{ab} v_1^{ab} (\vec{M}_1 \times \hat{h}) \sin B(x-x_2) \right] \cos V_g L \\
& \mp v_1^{ab} v_2^{ab} \left[(\vec{M}_1 \cdot \hat{h})(\vec{M}_2 \times \hat{h}) \left[1 - \cos B(x-x_1)\right] - (\vec{M}_2 \cdot \hat{h})(\vec{M}_1 \times \hat{h}) \left[1 - \cos B(x-x_2)\right] \right. \\
& \left. \left. + \vec{M}_1 \times \vec{M}_2 \right] \sin V_g L + u_1^{ab} u_2^{ab} \hat{h} \sin BL \sin V_g L \right\} \int_t e^{\boldsymbol{C}_{12}} \sin\left(\tfrac{1}{2}\boldsymbol{R}_{12}\right) \sin(Vt) \, ,
\end{aligned}
\tag{B4}
$$

where the $\mp$ sign correspond to lead 1,2 respectively.

One can verify that the spin current and spin density are not independent and are in fact related by the precessional equation of motion,

$$
\partial_t \vec{S} + \partial_x \vec{J}_s = -2\vec{h} \times \vec{S}.
\tag{B5}
$$

In the steady state, $\langle \partial_t \vec{S} \rangle = 0$, so one has

$$
\partial_x \langle \vec{J}_s(x) \rangle = -2\vec{h} \times \langle \vec{S}(x) \rangle.
\tag{B6}
$$

[1] A. G. Aronov, Pis'ma Zh. Eksp. **24**, 37 (1976), [JETP Lett. **24**, 32 (1976)].

[2] M. Johnson and R. H. Silsbee, Phys. Rev. Lett. **55**, 1790 (1985).

[3] M. Johnson, Phys. Rev. Lett. **70**, 2142 (1993).

[4] G. A. Prinz, Phys. Today **48 (4)**, 58 (1995).

[5] D. D. Awshalom and J. M. Kikkawa, Phys. Today **52 (6)**, 33 (1999).

[6] M. A. M. Gijs and G. E. W. Bauer, Adv. Phys. **46**, 285 (1997).

[7] C. H. Bennet and D. P. DiVicenzo, Nature (London) **404**, 247 (2000).

[8] L. Balents and R. Egger, Phys. Rev. Lett. **85**, 3464 (2000).

[9] L. Balents and R. Egger, Phys. Rev. B **64**, 035310 (2001).

[10] Q. Si, Phys. Rev. Lett. **78**, 1767 (1997).

[11] Q. Si, Phys. Rev. Lett. **81**, 3191 (1998).

[12] C. Bena and L. Balents, Phys. Rev. B **65**, 115108 (2002).

[13] K. Tsukagoshi, B. W. Alphenaar, and H. Ago, Nature (London) **401**, 572 (1999).

[14] W. Liang et al., Nature (London) **411**, 665 (2001).

[15] S. Datta, *Electronic Transport in Mesoscopic Systems* (Cambridge University Press, 1995).

[16] M. Bockrath et al., Nature (London) **397**, 598 (1999).

[17] Z. Yao, H. W. C. Postma, L. Balents, and C. Dekker, Nature (London) **402**, 273 (1999).

[18] Z. Yao, C. L. Kane, and C. Dekker, Phys. Rev. Lett. **84**, 2941 (2000).

[19] C. Dekker, Phys. Today **52 (5)**, 22 (1999).

[20] S. Tomonaga, Prog. Theor. Phys. **5**, 544 (1950).

[21] J. M. Luttinger, J. Math. Phys. **4**, 1154 (1963).

[22] F. D. M. Haldane, J. Phys. C **14**, 2585 (1981).

[23] F. D. M. Haldane, Phys. Rev. Lett. **47**, 1840 (1981).

[24] R. Egger and A. O. Gogolin, Phys. Rev. Lett. **79**, 5082 (1997).

[25] C. Kane, L. Balents, and M. P. A. Fisher, Phys. Rev. Lett. **79**, 5086 (1997).

[26] I. Safi and H. J. Schulz, Phys. Rev. B **52**, 17040 (1995).

[27] D. L. Maslov and M. Stone, Phys. Rev. B **52**, 5539 (1995).

[28] V. V. Ponomarenko, Phys. Rev. B **52**, 8666 (1995).

[29] J. Rammer and H. Smith, Rev. Mod. Phys. **58**, 323 (1986).

[30] C. Kane and M. P. A. Fisher, Phys. Rev. Lett. **72**, 724 (1994).

[31] C. Bena, S. Vishveshwara, L. Balents, and M. P. Fisher, Phys. Rev. Lett. **89**, 37901 (2002).

[32] S. Vishveshwara, C. Bena, L. Balents, and M. P. Fisher, Phys. Rev. B **66**, 165411 (2002).